Electronic Supplementary Material (ESI) for Journal of Materials Chemistry B.

Supplementary Information: Structural Transitions and Encapsulation Selectivity of Thermoresponsive Polyelectrolyte Complex Micelles

Sachit Shah[a] and Lorraine Leon[a, b, *]

a. Department of Materials Science and Engineering, University of Central Florida, Orlando, FL 32816, USA.

b. NanoScience Technology Center, University of Central Florida, Orlando, FL

* Corresponding Author: lorraine.leon@ucf.edu

pLK-Rhod MALDI-TOF Mass Spectroscopy

pLK-Rhod was synthesized by solid phase peptide synthesis using a rink amide resin solid support. L-lysine monomers were sequentially added, and finally carboxylic-terminated rhodamine ((5-(and-6)-Carboxytetramethylrhodamine)) monomer was coupled at the end of the molecule backbone. After lyophilization, an alpha-Cyano-4-hydroxycinnamic acid matrix was used with a MALDI 96-spot target plate (MSP 96 target ground steel, Bruker, Freemont, CA, USA). A Bruker Microflex LRF MALDI-TOF mass spectrometer (Fremont, CA, USA) was used to identify the molecular weight of the molecule.

The theoretical mass of the 28-residue L-lysine with rhodamine is about 3996 g/mol. From the mass spectroscopy plot below, the mass corresponds to the 28-residue L-lysine with rhodamine. All stoichiometric calculations for sample preparation were made using the actual mass and molar charge (1 cationic charge per lysine residue).

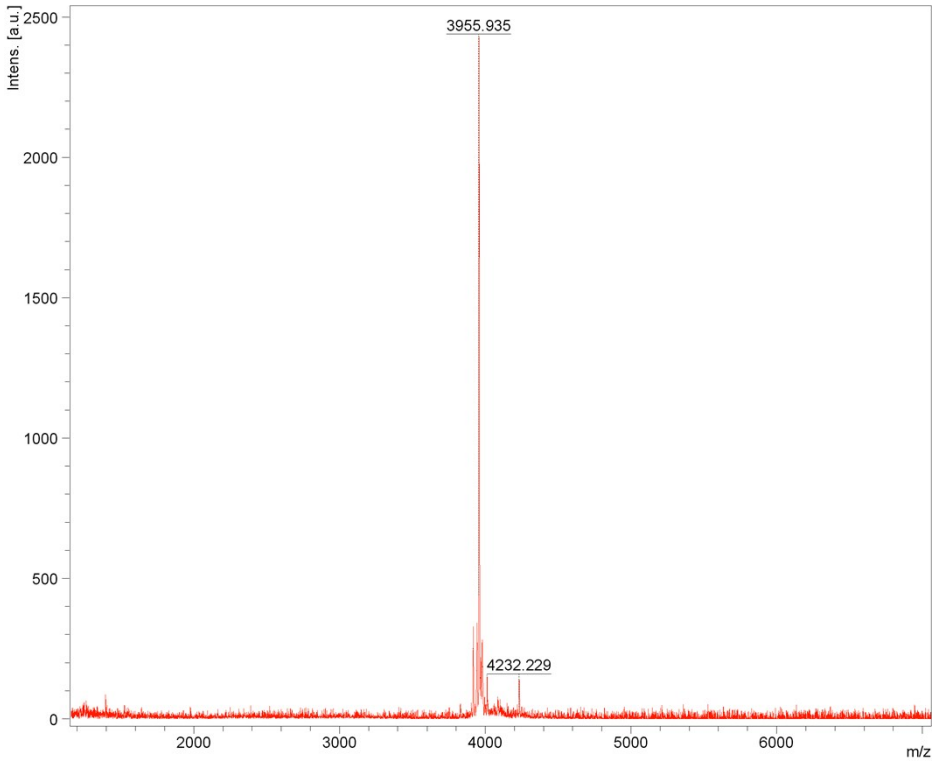

S 1. MADLI-TOF mass spectroscopy plot of pLK-Rhod. The reported mass corresponds to pLK_{28}-rhodamine.

pLK-Rhod Micelles DLS Data

S 2. DLS data of pLK-Rhod micelles. pLK-Rhod+DCP/HP micelles do not seem to show significant changes in scattering intensities, however, the pLK=-Rhod+DCP/DCP micelles show an increased scattering intensity and size, with increasing pLK-Rhod loading.

Sample	pLK-Rhod Concentration (%)	Temperature (°C)	Intensity (kcps)	Diameter (nm)	Polydispersity	Diffusion Coefficient (cm^2/s^{-1})
5% pLK-Rhod + DCP/HP	5	24	259.06 ± 0.27	-	-	8.139E-8 ± 5.185E-10
10% pLK-Rhod + DCP/HP	10		208.66 ± 0.74	-	-	8.807E-8 ± 7.510E-10
30% pLK-Rhod + DCP/HP	30		237.73 ± 0.75	-	-	8.559E-8 ± 4.858E-10
50% pLK-Rhod + DCP/HP	50		210.46 ± 1.10	-	-	9.258E-8 ± 3.681E-10
5% pLK-Rhod + DCP/DCP	5		37.84 ± 0.23	31.7 ± 0.2	0.098 ± 0.039	1.530E-7 ± 1.098E-9
10% pLK-Rhod + DCP/DCP	10		38.47 ± 0.47	31.8 ± 0.2	0.087 ± 0.026	1.527E-7 ± 1.134E-9
30% pLK-Rhod + DCP/DCP	30		46.33 ± 0.29	34.9 ± 0.1	0.206 ± 0.013	1.392E-7 ± 6.944E-10
50% pLK-Rhod + DCP/DCP	50		87.47 ± 0.25	42.5 ± 0.2	0.121 ± 0.004	1.141E-7 ± 4.190E-10

SAXS Modelling

The incoherent scattering data was background-subtracted using the scattering of the solvent to obtain the scattering caused by the particles only. The scattering length density (SLD) values for the individual micelle components are very similar (Table S3). Therefore the SLD for both systems was calculated as a monomer weighted average of the components. The SLD values were calculated using the APS Irena Package with Igor Pro. The SLD for the DCP/HP system and DCP/DCP system used were 10.2374×10^{-6} Å^{-2} and 10.1627×10^{-6} Å^{-2}, respectively.

S 3. Scattering length densities of micelle components calculated using Scattering Contrast Calculator tool of the APS Irena package.

Component	Scattering Length Density ($\times 10^{-6}$ Å^2)
Water	9.42
pLK	10.19
pAA	10.29
pNIPAM	10.23
pEG	10.11

The fitting model for each system was selected based on the confirmation of morphology from the TEM and the effectiveness of each fitting model to the same system at different polymer concentrations. A cylinder with a polydisperse radius form factor was used to fit the data for the DCP/HP system as shown in Figure S4. Tables S5 shows the corresponding fitting parameters obtained. As it can be seen, the sizes for the particles at varying concentrations do not change significantly. The scale factor increases for increasing polymer concentration since the intensity of scattering increases due to formation of more particles, confirming the formation of equilibrium structures. The DCP/HP system was also fit using an elliptical cylinder form factor (Figure S6) and similar results were found (Table S7). For the DCP/DCP system, Gaussian sphere, log normal sphere, and Schulz sphere models were used to fit the data shown in Figures S8, S10, and S12 respectively, with the parameters for fitting shown in corresponding Tables S9, S11, and S13. Three concentrations for the DCP/DCP system were not tested due to limited allotment of beamtime.

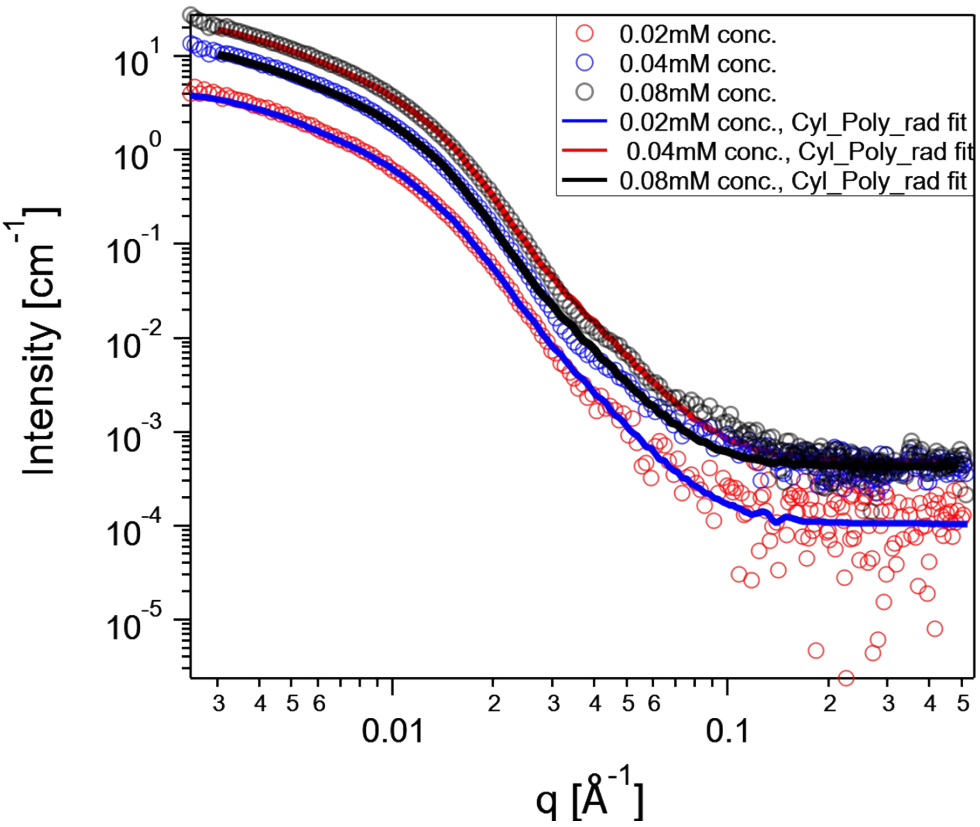

S 4. SAXS data for DCP/HP system at 24°C for three polymer concentrations – 0.02 mM, 0.04 mM, and 0.08 mM, using a Cylinder with Polydisperse Radius fit.

S 5. Cylinder with Polydisperse Radius fitting parameters for the DCP/HP system at 0.02 mM, 0.04 mM, and 0.08 mM concentration.

Sample	**DCP/HP**		
Concentration (mM)	0.02	0.04	0.08
Scale	9.048E-04	2.62E-03	5.216E-03
Radius (Å)	114.74	122.67	119.71
Length (Å)	1121.79	1218.61	1191.52
Polydispersity	0.363	0.318	0.310
Background (cm^{-1})	1.044E-04	4.252E-04	4.805E-04
Scale Error	6.175E-06	8.41E-06	1.227E-05
Radius Error	1.091E+00	4.085E-01	2.616E-01
Length error	23.43	10.68	6.21
Polydispersity error	9.318E-03	3.285E-03	2.094E-03
Background error	1.338E-05	1.327E-05	1.329E-05
χ^2	100.44	434.56	899.66

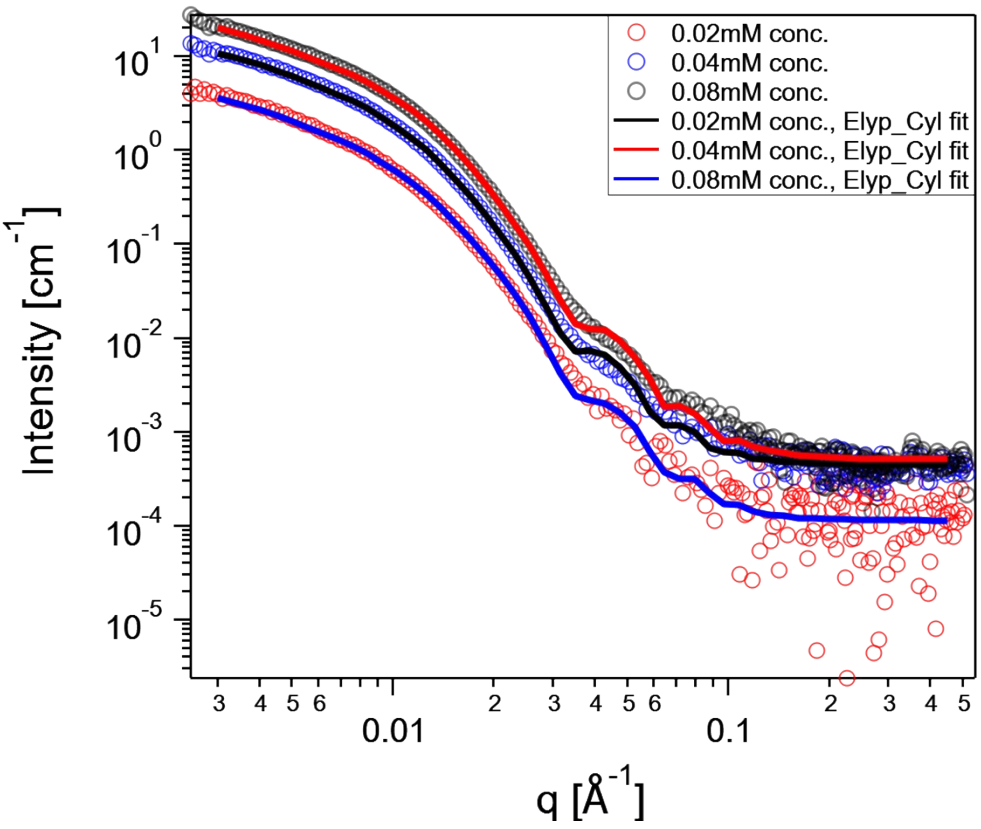

S 6. SAXS data for DCP/HP system at 24°C for three polymer concentrations – 0.02 mM, 0.04 mM, and 0.08 mM, using an Elliptical Cylinder fit.

S 7. Elliptical Cylinder fitting parameters for the DCP/HP system at 0.02 mM, 0.04 mM, and 0.08 mM concentration.

Sample	**DCP/HP**		
Concentration (mM)	0.02	0.04	0.08
Scale	8.811E-04	2.577E-03	5.124E-03
Minor Radius (Å)	101.86	106.27	102.95
ν = major/minor radii	2.201	2.088	2.042
Length (Å)	1321.75	1306.45	1358.42
Background (cm^{-1})	1.133E-04	4.423E-04	5.094E-04
Scale Error	5.692E-06	8.356E-06	1.198E-05
Minor Radius Error	5.258E-01	2.381E-01	1.528E-01
ν error	3.305E-02	1.351E-02	8.632E-03
Length error	32.25	11.88	7.83
Background error	1.336E-05	1.326E-05	1.33E-05
χ^2	131.83	303.66	860.30

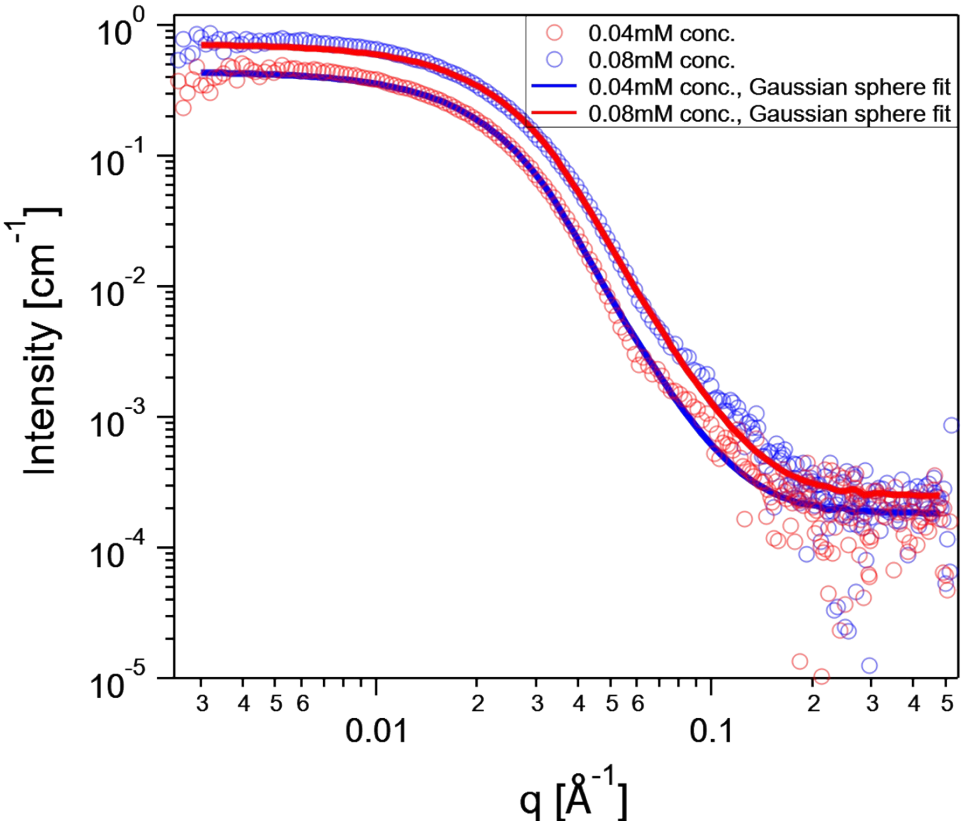

S 8. SAXS data for DCP/DCP system at 24°C for two polymer concentrations – 0.04 mM and 0.08 mM, using a Gaussian Sphere fit.

S 9. Gaussian Sphere fitting parameters for the DCP/DCP system at 0.04 mM and 0.08 mM concentration.

Sample	**DCP/DCP**	
Concentration (mM)	0.04	0.08
Volume Fraction	2.818E-03	5.651E-03
Mean Radius (Å)	35.692	23.510
Polydispersity (σ/average)	0.909	1.377
Background (cm^{-1})	1.834E-04	2.483E-04
Scale Error	8.939E-06	7.486E-05
Mean Radius Error	2.213	1.584
Polydispersity error	7.549E-02	1.118E-01
Background error	1.347E-05	1.355E-05
χ^2	189.08	478.25

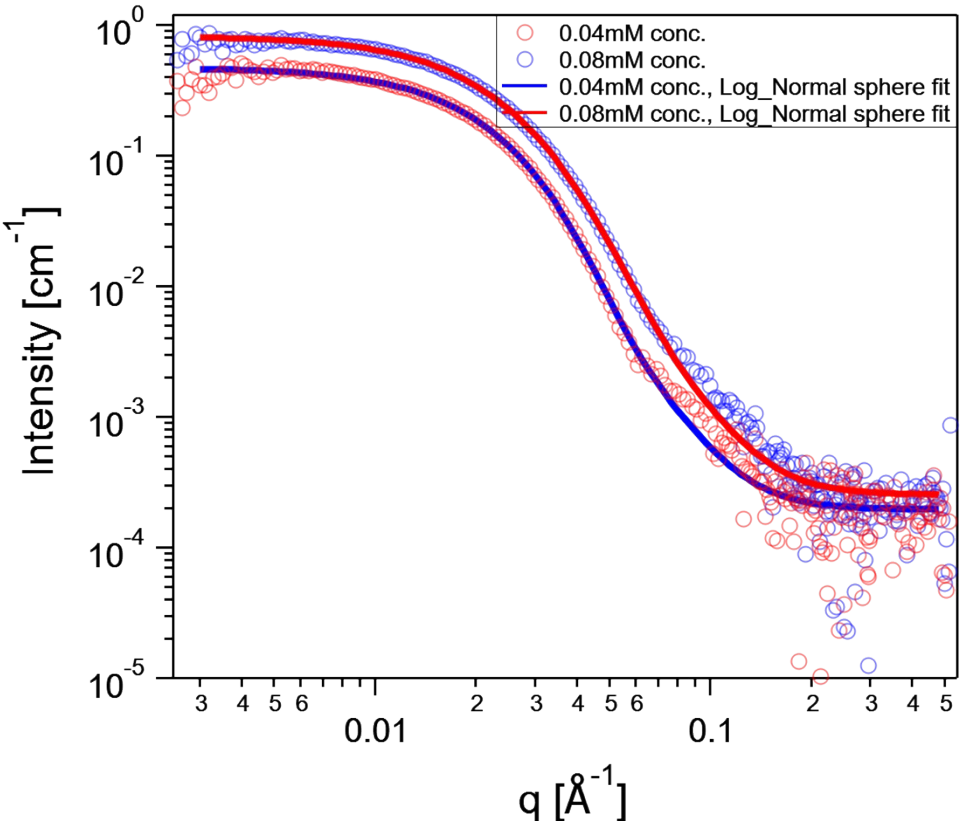

S 10. SAXS data for DCP/DCP system at 24°C for two polymer concentrations – 0.04 mM and 0.08 mM, using a Log Normal Sphere fit.

S 11. Log Normal Sphere fitting parameters for the DCP/DCP system at 0.04 mM and 0.08 mM concentration.

Sample	**DCP/DCP**	
Concentration (mM)	0.04	0.08
Volume Fraction	2.783E-03	7.411E-05
Median Radius (Å)	60.333	49.758
σ	0.300	0.342
Background (cm^{-1})	1.961E-04	2.538E-04
Scale Error	1.111E-05	1.909E-07
Radius Error	0.508	0.306
σerror	3.679E-03	2.370E-03
Background error	1.342E-05	1.351E-05
χ^2	109.94	178.28

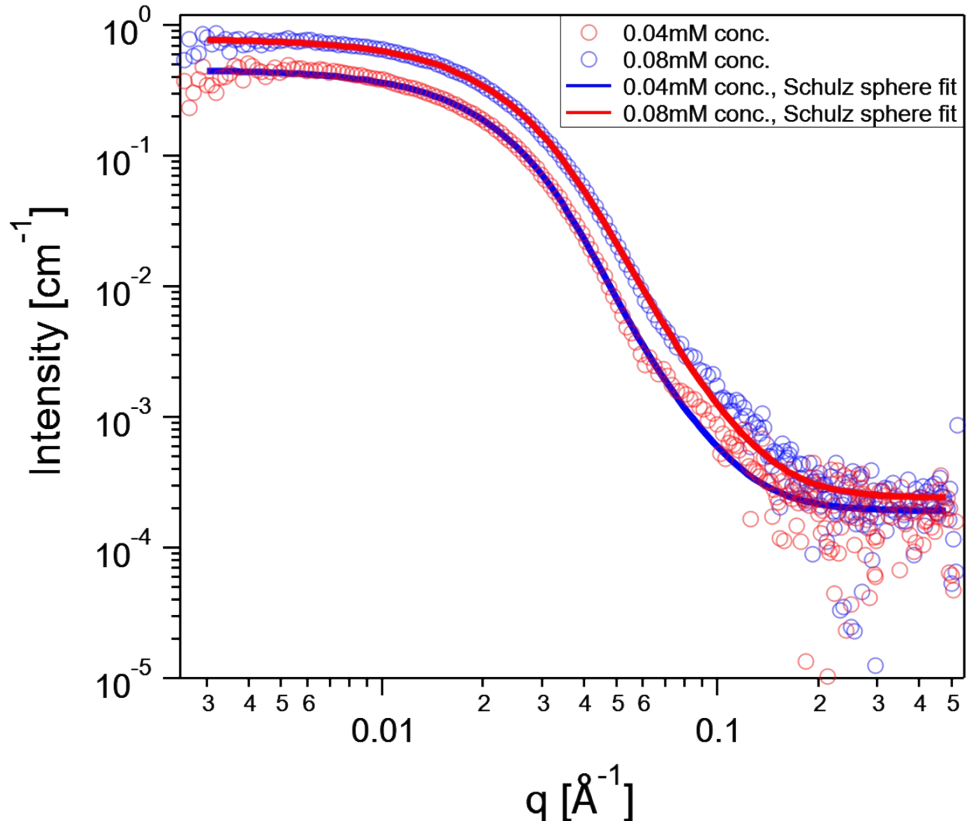

S 12. SAXS data for DCP/DCP system at 24°C for two polymer concentrations – 0.04 mM and 0.08 mM, using a Schulz Sphere fit.

S 13. Schulz Sphere fitting parameters for the DCP/DCP system at 0.04 mM and 0.08 mM concentration.

Sample	**DCP/DCP**	
Concentration (mM)	0.04	0.08
Volume Fraction	2.809E-03	7.526E-05
Mean Radius (Å)	58.674	46.071
Polydispersity (σ/average)	0.361	0.447
Background (cm^{-1})	1.912E-04	2.402E-04
Scale Error	1.212E-05	2.150E-07
Mean Radius Error	0.656	0.444
Polydispersity error	6.420E-03	5.225E-03
Background error	1.345E-05	1.355E-05
χ^2	133.67	207.36

Micelle Size from TEM Images

The TEM images were analyzed manually using ImageJ software to measure the sizes of the micelles. Measurements of 18 micelles were made and are reported below (Table S14). The lengths of the DCP/HP micelles were not possible to determine due to entangling of the particles, and hence only the diameters of the particles are reported. The range in measurement values for the DCP/HP micelles may be attributed to the orientation of an elliptical cross-section. The range in measurement values for the DCP/DCP micelles is attributed to aggregation and overlapping clusters of spherical micelles.

S 14. List of size measurements using ImageJ software of particles from TEM images for both systems.

	Sample	Diameter (nm)
1.	DCP/HP System	20.3
2.		20.8
3.		20.8
4.		26.1
5.		27.3
6.		28.3
7.		23.1
8.		22.5
9.		27.3
10.		19.9
11.		31.5
12.		30.2
13.		23.0
14.		21.3
15.		24.4
16.		25.4
17.		28.9
18.		21.0
Average		*24.6*

	Sample	Diameter (nm)
1.	DCP/DCP System	20.4
2.		23.3
3.		21.4
4.		17.7
5.		21.7
6.		17.2
7.		17.6
8.		16.5
9.		14.7
10.		20.8
11.		17.5
12.		17.5
13.		16.6
14.		16.5
15.		21.0
16.		15.7
17.		17.6
18.		17.0
Average		*18.4*

Disrupting H-bonding between pNIPAM and pAA with Urea

As mentioned in the main article, there is irreversibility in the scattering intensities of the micelles after a heat cycle. We hypothesize that this may be due to H-bonding between the two blocks of the pNIPAM-pAA, which increases as the pNIPAM transitions to its hydrophobic state and may persist upon cooling. To test this hypothesis, urea is used to disrupt these H-bonds, and the reversibility of the DCP is then investigated using dynamic light scattering. A 0.02 mM pNIPAM-pAA solution was made, and three samples with 500 mM, 1000 mM, and 1500 mM urea were prepared. At elevated temperatures, the DCP would form amphiphilic micelles, with a pNIPAM hydrophobic core, and a pAA hydrophilic corona. The intensity of scattering was recorded at 50 ^{o}C after heating the samples to the temperature in an oil bath for one hour. The samples were allowed to cool for one hour, after which they were heated once more to 50 ^{o}C for an hour and the intensity of scattering was

recorded for the second time. The scattering intensity data for the particles with varying concentrations of urea is shown in Table S15.

S 15. DLS reversibility data for pNIPAM-pAA with and without urea to illustrate that disruption of H-bonding aides in the reversibility of the structures formed when pNIPAM-pAA is heated past the LCST. This is seen by the constant scattering intensity, before and after a heat-cycle when urea is added.

Sample	Polymer Concentration (mM)	Urea Concentration (mM)	Temperature (°C)	Intensity (kcps)	Diameter (nm)	Polydispersity	Diffusion Coefficient (cm^2/s^{-1})
pNIPAM-pAA - Pre heat cycle	0.02	0	50	261.58 ± 6.63	172.9 ± 1.6	0.06 ± 0.010	4.950E-08 ± 5.752E-10
		500		309.10 ± 6.52	199.9 ± 0.6	0.065 ± 0.022	4.283E-08 ± 1.668E-10
		1000		296.75 ± 3.98	194.9 ± 4.7	0.029 ± 0.070	4.394E-08 ± 1.352E-9
		1500		294.59 ± 4.66	193.9 ± 1.6	0.036 ± 0.033	4.415E-08 ± 3.704E-10
pNIPAM-pAA - Post heat cycle	0.02	0		281.82 ± 2.19	121.7 ± 1.1	0.019 ± 0.011	4.899E-08 ± 1.506E-10
		500		318.54 ± 3.15	195.7 ± 2.3	0.02 ± 0.036	4.443E-08 ± 6.023E-10
		1000		293.81 ± 9.44	193.6 ± 0.5	0.046 ± 0.014	4.714E-08 ± 2.546E-10
		1500		282.84 ± 2.35	192.3 ± 1.6	0.026 ± 0.020	4.977E-08 ± 3.356E-10

MB Dialysis to show no encapsulation within PEC Micelles

A 3.5-5 kDa cutoff dialysis tube was used to dialyze the pure MB and MB samples for 72 hours. As seen from the UV-absorption spectra in S16a-d, the absorption of pure MB and the two micelle systems with MB decreases correspondingly over time. The MB with pNIPAM-pAA also decreases in overall absorption intensity, however with a decrease in trimers, an increase in monomer is observed at certain time points. Table S17 shows the loss of trimers, dimers and monomers over time for each sample, calculated by a loss in absorption intensity. The negative values for the loss of monomer for the pNIPAM-pAA samples indicate an increase in monomers, as seen in S16b. This experiment confirms that there was no encapsulation of MB because a similar loss profile is observed for pure MB and both micelle systems.

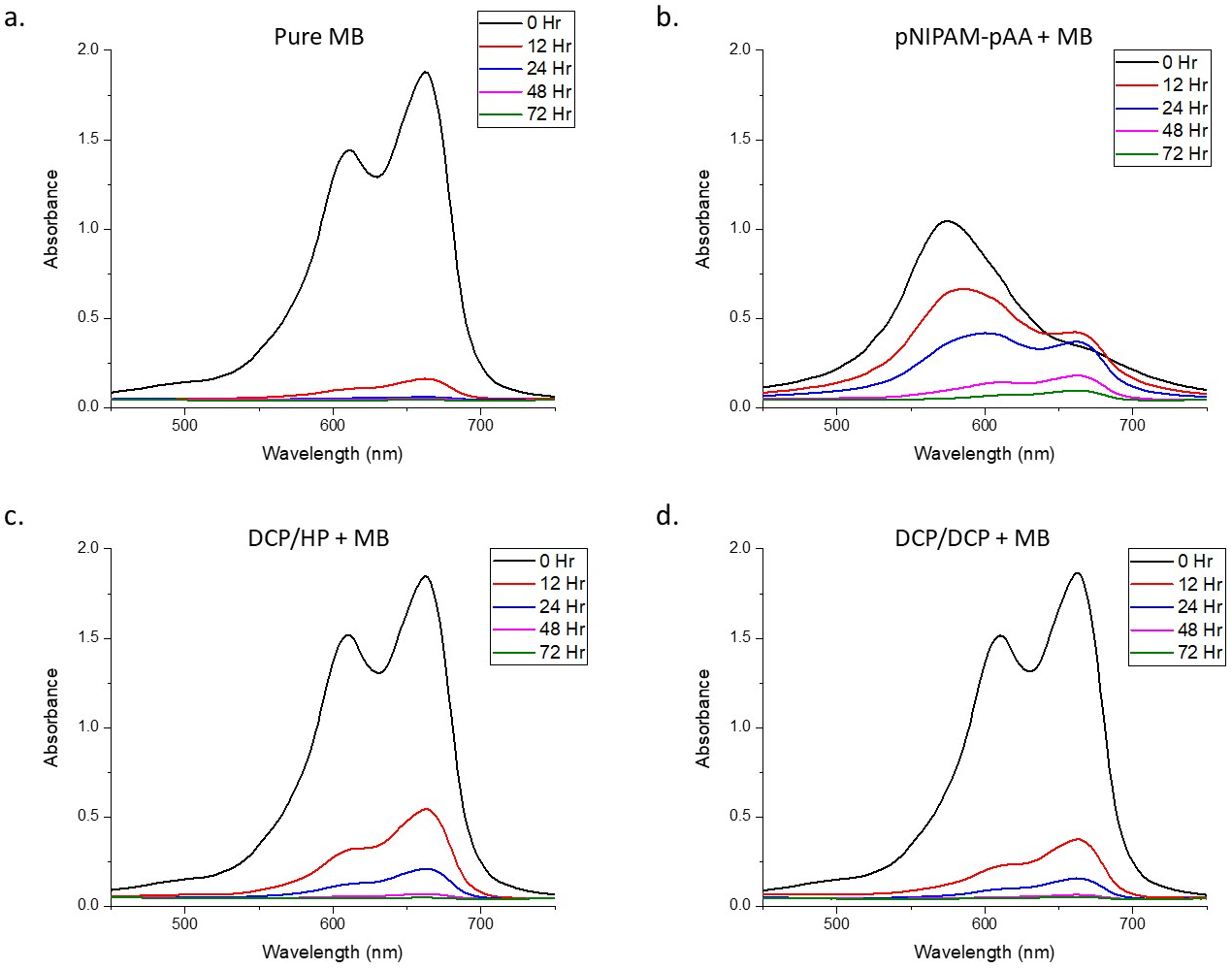

S 16. Absorption spectra of pure MB (a.), pNIPAM-pAA + MB (b.), DCP/HP + MB (c.), and DCP/DCP + MB (d.) showing decreasing intensity over time. This indicates that there was no encapsulation as the MB molecules diffuse out of the sample over time.

S 17. Table showing the loss of MB trimers, dimers, and monomers for each sample during 72 hours of dialysis calculated from S16.

Sample	Time (Hr)	Loss of Trimer % Compared to 0 Hr	Loss of Dimer % Compared to 0 Hr	Loss of Monomer % Compared to 0 Hr
Pure MB	0	-	0.0	0.0
	12	-	92.6	91.4
	24	-	96.4	96.8
	48	-	96.8	97.3
	72	-	97.1	97.7
pNIPAM-pAA + MB	0	0.0	0.0	0.0
	12	37.7	19.2	-22.4
	24	64.8	43.4	-7.3
	48	90.4	80.0	47.5
	72	95.0	90.1	72.0
DCP/HP + MB	0	-	0.0	0.0
	12	-	78.9	70.6
	24	-	91.7	88.6
	48	-	96.4	96.3
	72	-	97.0	97.4
DCP/DCP + MB	0	-	0.0	0.0
	12	-	84.9	79.9
	24	-	93.6	91.7
	48	-	96.6	96.6
	72	-	97.0	97.2

MB samples fluorescence intensities

Fluorescence intensities of pure MB compared to MB with pNIPAM-pAA, DCP/HP, and DCP/DCP. There is no quenching of intensity of MB with the two micelle systems, while there is some degree of quenching of MB fluorescence with pNIPAM-pAA. This data comparable to the UV-absorption spectra.

S 18. Table showing the fluorescence intensities of pure MB and MB with pNIPAM-pAA, DCP/HP, and DCP/DCP.

Pure MB	pNIPAM-pAA + MB	DCP/HP + MB	DCP/DCP + MB
9580 ± 299	7708 ± 205	9977 ± 88	9396 ± 190

* Fluorescence intensities reported in RFU

pLK-Rhod DCP/HP & DCP/DCP Micelles Absorbance

The absorption spectra of pure pLK-Rhod, and encapsulated pLK-Rhod in DCP/HP and DCP/DCP are shown below in Figure S20. As with the fluorescence intensities of these samples, the degree of quenching is higher at higher pLK-Rhod loading amounts.

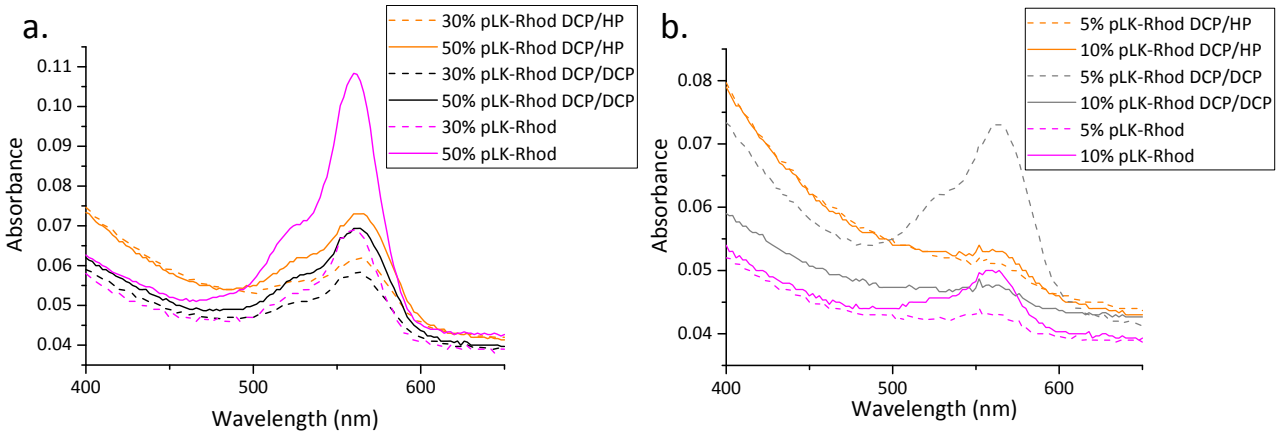

S 19. Absorbance spectroscopy of a. 30% and 50% pLK-Rhod micelles and b. 5% and 10% pLK-Rhod micelles.

Separation of free pLK-Rhod from encapsulated pLK-Rhod in DCP/HP and DCP/DCP

A 30 kDa cutoff Amicon centrifugal separation tube was used to separate free (unencapsulated) pLK-Rhod from the pLK-Rhod with the two micelle systems. This was done to calculate the loading amount of the polyion cargo in the micelles. Under the same centrifugation conditions of 7500 xg for 20 minutes, it was seen that the pure pLK-Rhod filtered from the sample had a lower fluorescence intensity as compared to the initial sample. This loss was attributed to uptake by the separation membrane. For more accurate comparison, it was assumed that the degree of uptake by the membrane would remain constant, and so the fluorescence intensities of the filtrates of the pLK-Rhod loaded micelles were compared to the intensities of the filtrates of pure pLK-Rhod of the same concentration. Table S20 below shows the calculated loading amounts (in percentage values) of the pLK-Rhod in each case. A higher concentration of pLK-Rhod leads to a higher loading %.

S 20. Table showing the loading or encapsulation amount of pLK-Rhod in each sample.

Sample	pLK-Rhod concentration (cationic charge %)	Loading Amount (%)
DCP/HP + pLK-Rhod	5	84.7
	10	88.2
	30	90.0
	50	90.8
DCP/DCP + pLK-Rhod	5	66.3
	10	76.8
	30	83.2
	50	80.3

Micelle Post-transition Solution Turbidity

To confirm that post-transition micelle solution turbidity would not impact fluorescence intensity measurements, 100 μL volume of 0.04 mM and 0.08 mM polymer concentration micelle solutions were heated to 50^{o}C for 90 minutes and their absorbance was measured at 800 nm. A marginal increase from 0.038 to 0.047 absorbance units was seen.

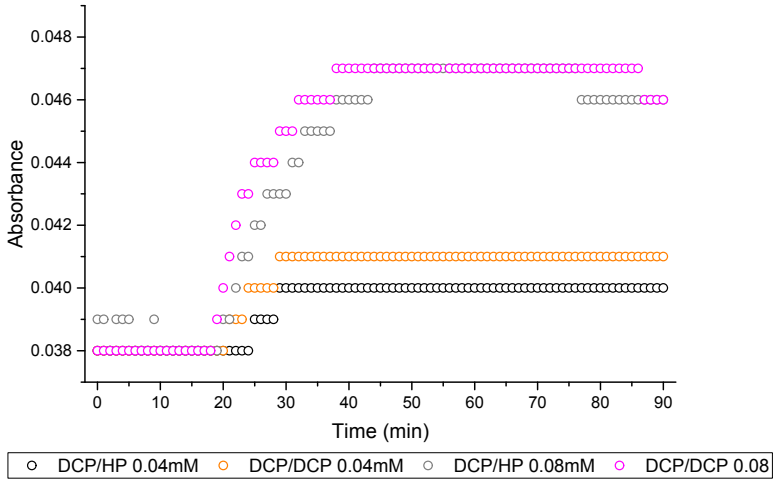

S 21. Absorbance intensity over time while heating DCP/HP and DCP/DCP micelles at 0.04 mM and 0.08 mM concentration to 50°C.

pLK-Rhod Reversibility

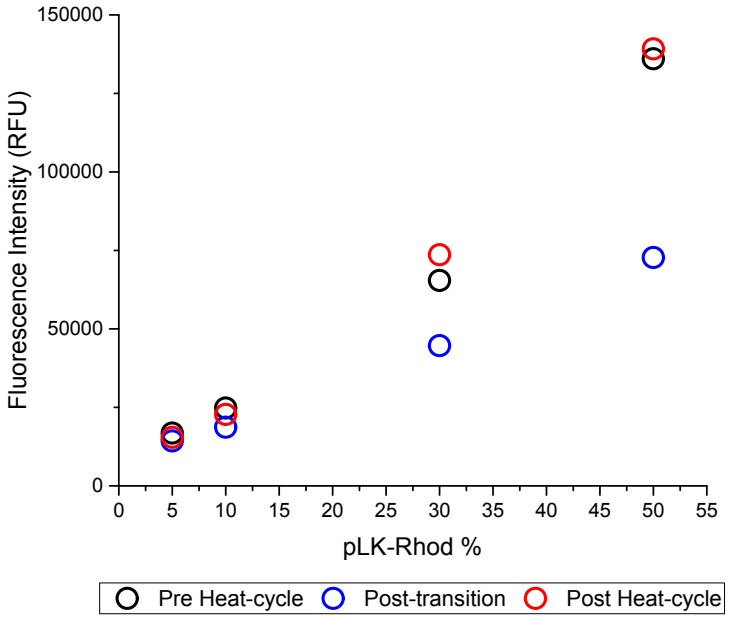

S 22. Fluorescence intensity of pure pLK-Rhod under cyclic heating shows decreased intensity when heated, but the intensity is recovered when re-cooled.